Elastic Scattering of Heavy Ions from Several Gas Targets*

E. NEWMAN,† P. G. ROLL,‡ AND F. E. STEIGERT
Yale University, New Haven, Connecticut

(Received February 13, 1961)

The absolute differential cross section for the elastic scattering of oxygen by gaseous targets of helium, nitrogen, and neon and of carbon by nitrogen were measured from about 4 to ~20 degrees in the center-of-mass system. The energy of the incident heavy ions was ~10 Mev per atomic mass unit. The ratio of the elastic cross section to the Coulomb cross section exhibits diffraction-like oscillations which damp out as $\eta=Z_1Z_2e^2/\hbar v$ increases from ~1 to ~4. The results are compared with the predictions of a simple diffraction model, a sharp-cutoff model, and a modified-cutoff model. Reasonably good agreement is obtained in predicting the angular position of the maxima and minima, but not the absolute cross section. The modified-cutoff model appears to apply only if η is greater than about 2.5. The value of r_0 found for the O^{16}—Ne scattering is 25% greater than for the remaining three reactions.

INTRODUCTION

IN the past years much attention has been given to the experimental investigation of elastic scattering cross sections. Recently, data for the scattering of alpha particles and of heavier ions has been accumulated rapidly with a view toward inferring the properties of nuclear matter.

Angular distributions for elastic scattering have been analyzed in terms of sharp-cutoff[1–3] or modified-sharp-cutoff[4] models, by optical model calculations,[5] and in terms of the rainbow model.[6] Since most angular distributions in which the parameter $\eta=Z_1Z_2e^2/\hbar v$ is less than ~5 exhibit a diffraction-like structure,[7] these experiments are amenable to analysis by a simple diffraction model.[8] In this expression Z_1 and Z_2 are the incident and target nuclear charge, respectively, v is the relative velocity of the two particles, e is the electronic charge, and $\hbar$ is Planck's constant divided by 2π.

A mean interaction radius may be obtained from each of these models. In addition, the modified-sharp-cutoff, optical, and rainbow models allow a parametrization of the shape of the potential so that information on the diffuseness of the nuclear edge may be inferred. The rainbow model is applicable only to data which exhibit a smooth dropoff from the Coulomb cross section with increasing angle. Calculations by Porter[9] and more recently by Bassel, Drisko, and Melkanoff[10] with the optical model have met with a fair degree of success.

The present differential cross sections were measured for the elastic scattering of O^{16} from He^4, N^{14}, and Ne^{20}; and of C^{12} from N^{14}. They are part of a continuing series to determine the interaction radii of heavy-ion interactions in a region of the periodic table where relatively large changes might be expected. They also provide a test of the applicability of the modified-sharp-cutoff model.

EXPERIMENTAL APPARATUS

At energies of 10 Mev per nucleon the cross section for elastic scattering from low-Z targets deviates markedly from Coulomb scattering very close to the forward direction. These measurements, therefore, presented the usual problems of dealing with gas targets, plus the added complications of determining the cross sections at small angles. Figure 1 is a view of the scattering apparatus (the section is taken in the plane of scattering). The detector rotates about the center of the target volume which is located within a standard 4-in. diam Sylphon bellows. Keeping both faces of the bellows perpendicular to the plane of rotation, alternate sides undergo simple compression and expansion without torsion. This arrangement has a total angular sweep of approximately 100 deg. As shown in the figure, the midpoint of the swing used here is 30°; this permits the angular distributions to be followed continuously from −20° to +80° in the laboratory system.

The beam enters the collimating system through a 2.4-mg/cm² nickel foil. This foil serves the dual purpose of keeping the target gas within the chamber and of providing a diffuse source of particles entering the collimators. The collimating apertures and antiscat-

* Work performed under the auspices of the U.S. Atomic Energy Commission. This article is based on a dissertation submitted by E. Newman in partial fulfillment of the requirements for the degree of Doctor of Philosophy at Yale University.

† Socony Mobil Fellow. Now at the Electronuclear Research Division, Oak Ridge National Laboratory, Oak Ridge, Tennessee.

‡ Now at the Palmer Physical Laboratory, Princeton University, Princeton, New Jersey.

[1] A. Akhieser and I. Pomeranchuk, J. Phys. (U.S.S.R.) **9**, 471 (1945).

[2] E. Clementel and A. Coen, Nuovo cimento **10**, 988 (1953).

[3] J. S. Blair, Phys. Rev. **95**, 1218 (1954); *ibid.* **108**, 827 (1957).

[4] J. A. McIntyre, K. H. Wang, and L. C. Becker, Phys. Rev. **117**, 1337 (1960).

[5] A rather complete list of references is given in the *Proceedings of the International Conference on the Nuclear Optical Model, Florida State University Studies No. 32*, edited by A. E. S. Green, C. E. Porter, and D. S. Saxon (The Florida State University, Tallahassee, 1959).

[6] K. W. Ford and J. A. Wheeler, Ann. Phys. **7**, 259 (1959).

[7] J. A. McIntyre, S. D. Baker, and T. L. Watts, Phys. Rev. **116**, 1212 (1959).

[8] G. Placzek and H. A. Bethe, Phys. Rev. **57**, 1075 (1940).

[9] C. E. Porter, Phys. Rev. **112**, 1722 (1958).

[10] R. H. Bassel, R. M. Drisko, and M. A. Melkanoff, Bull. Am. Phys. Soc. **5**, 67 (1960).

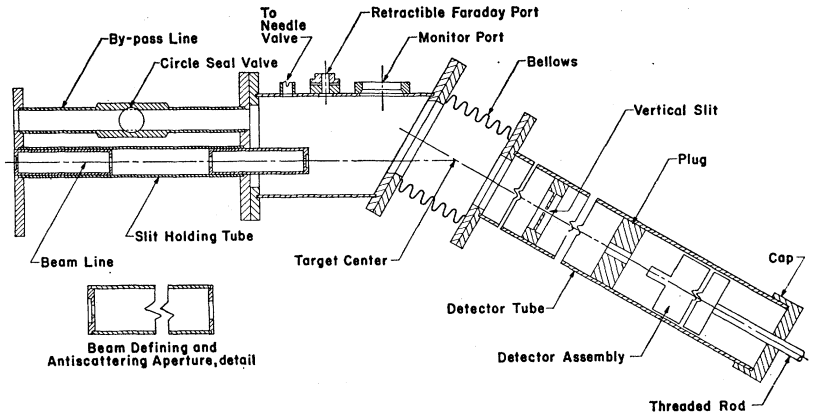

FIG. 1. View of the scattering apparatus. The section is in the plane of scattering. The beam enters the collimating apertures through a Ni foil. The detector tube rotates on the edge of a 33-in. diameter pulley wheel (not shown). The center of rotation is at the point marked "target center." The angular range of the detector arm is from $-20°$ to $+80°$.

tering apertures are machined into opposite ends of a brass tube 10 cm long. Two such assemblies are placed in the slit-holding tube. Two pairs of beam-defining apertures were used, first a 0.200-in. diam set, and a second 0.062-in. diam set for small-angle measurements. In both cases the antiscattering apertures are $\frac{1}{4}$ in. in diameter. The distance between the circular defining apertures is 30 cm.

As the beam emerges from the second collimating aperture it enters a 4-in. diam tube. As may be noted, the beam does not pass down the axis of the tube but is 0.600 in. off center to allow the target volume to remain in the center of the bellows. There are several entrances to this tube, (1) the gas inlet needle valve, (2) a target pressure gauge port, (3) a monitor port, and (4) a port for a retractable Faraday cup. This Faraday cup may be slid into place immediately following the second defining aperture. This indicates that the heavy-ion beam is entering the chamber, and provides an estimate of the current. The cup may then be withdrawn to a position where the bottom is approximately one inch from the beam center line. When in this position, a positive bias is applied and the signal derived from electron pickup is used for machine tuning purposes.

The detector tube, a 3-in. o.d. seamless stainless steel tube 5 ft long, follows the bellows; it contains the rectangular slit and the detector assembly. This tube rotates on the edge of a 33-in. diam pulley wheel (not shown in Fig. 1) with the hub as a center. The edge of the wheel was ground to provide a smooth flat surface.

The alignment of the components was accomplished by means of a standard surveyors' transit. The detector tube was set at the zero angle of scattering and all apertures centered on a common line passing through the axis of rotation. The long sides of the rectangular aperture could be made vertical by rotating the detector arm slightly off the zero-angle position such that the transit vertical cross hairs coincided with the side of the aperture.

Either of two interchangeable circular apertures of 200 mils or 62 mils diameter were placed in front of the detector. The width of the rectangular slit was 64 mils and its height great enough so that the detector encompassed the entire beam in cross section. The beam volume thus defined is the intersection of cones and pyramids. Figure 2 shows schematically the geometric configuration of the apertures and target volume. In Table I are listed the dimensions referred to in the figure.

The detector for the elastically scattered particles was a thin NaI(Tl) crystal mounted directly to the face of a DuMont 6292 photomultiplier. A housing was constructed with the vacuum seal made directly to the face of the phototube to permit the hygroscopic crystal to be kept under vaccum continuously. The target-to-detector distance could be adjusted with a threaded rod connected to the detector assembly and plug. Once the detector had been positioned and the chamber

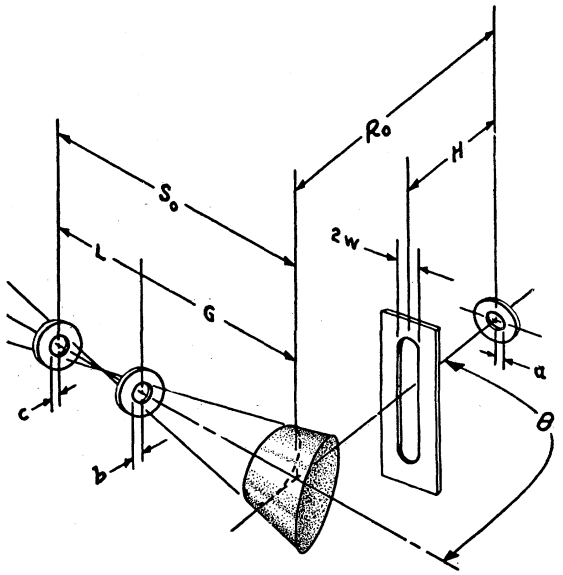

FIG. 2. Schematic representation of the scattering geometry. For appropriate dimensions see Table I. The dimensions have not been drawn to scale for reasons of clarity. The notation is that of reference 12.

TABLE I. Dimensions (cm) referred to in Fig. 2.

Quantity	2°–5°	3.5°–10°
a	0.0787	0.254
b	0.0787	0.254
c	0.0787	0.254
$2w$	0.163	0.163
R_0	77.72	50.80
L	30.00	30.00
S_0	45.72	45.72
G	15.72	15.72
H	51.82	38.10

evacuated and filled with target gas, a Circle Seal valve was opened to expose the detector to the target volume. In this manner the NaI was kept protected against moisture without the use of packaging or windows.

The elastic detector signal was analyzed by a 20-channel pulse height analyzer. A 400-channel analyzer was also available and was used in addition to the former to obtain spectra for some of the runs at large angles. Although limited in number of channels and readout, the 20-channel analyzer was more useful because it required smaller dead time corrections.

The scattering angle was measured from an angular vernier table rescued from a small optical spectrometer. It was possible, by means of a low-power hand lens, to read the angle to $\pm\frac{1}{4}$ minute. The zero-degree point was determined from the symmetry of the left-right scattering yields. The difference between the optical method of determining zero degrees and this method was never greater than 0.1 deg.

Scattered particles were monitored to determine the exposure during a given run. These were detected by a 1-mm thick CsI crystal mounted to a DuMont 6467 photomultiplier. A 2.2-mg/cm^2 Ni foil was placed in front of the detector to screen out particles of very low energy. The angular acceptance of the monitor was restricted to the angles from 60° to 170° by use of a collimator.

After the monitor signal had been amplified, it was fed to an integral discriminator. The output of the discriminator was used to drive a scaler, the count switch of which also actuated the 20-channel elastic particle analyzer.

To calibrate the monitor a series of measurements were made in which the beam was collected in a Faraday cup. The elastic detector was removed, the detector arm set at zero degrees, and the cup installed in the end of the arm. The Faraday cup itself was located in a chamber with an aluminum foil entrance window. The cup was insulated from the housing with two Teflon pillars. A ring magnet was positioned in front of the collection cup and a 4-kv negative potential was applied to it to suppress secondary electrons arriving from the cup or window. The operating pressure within the Faraday chamber was maintained below 5×10^{-6} mm Hg to minimize any ionization chamber effect within the housing. The number of monitor counts per collected microampere of beam was constant for suppressor voltages from 0.5 to 4.0 kv. To determine the loss of integrated beam due to multiple scattering, the number of monitor counts per microampere was measured as a function of target pressure. Varying the pressure from 10 to 75 mm Hg resulted in no detectable effect. An upper limit of 1% has been placed on this source of error. In making the absolute calibration, sufficient counts were recorded on the monitor scaler to obtain 1% statistics.

Standard commercial grade dry nitrogen and research grade helium and neon gases were used as targets. The gas was present in the chamber from the entrance window to the elastic particle detector. To insure as low contamination as possible, the gas was continuously flowed through the chamber at a typical rate of 1 to 2 cc/min. A pressure of 50.0 mm Hg, measured with a Wallace and Tiernan 0–200 mm pressure gauge, was held constant with a Manostat.[11] The gas temperature was assumed to be that of the surroundings and, therefore, the ambient temperature was used in calculating the target density. The error in density is estimated to be $\pm1\%$.

PROCEDURE

The heavy-ion beams of O^{16} and C^{12} used in this experiment were accelerated to a nominal energy of 10 Mev per nucleon in the Yale heavy-ion linear accelerator. At the exit of the accelerating cavity a pair of quadrupole magnets focused the beam; it was then magnetically analyzed to approximately 1% in energy, passed through a bending magnet so that it was again parallel to the original direction, and focused once again with a pair of quadrupoles.

Before data were taken, the lower level in the monitor discriminator was set; this value was selected to be in a region of pulse height where the slope of the monitor spectrum was not rapidly varying.

The small beam-defining and detector apertures were used in the 2° to 5° (laboratory) angular region, the large set of apertures from 3.5° to ~10°. This provided an overlap of approximately 2° for the two systems. The angular resolutions in the laboratory for the two systems are 0° 13′ and 0° 25′, respectively (full width at half-maximum). The angular interval used for the "small" angle geometry was 0° 10′; for the "large" angle measurements data were taken at 0° 15′ intervals. The scattering of O^{16} by He was the exception, the intervals used here were 0° 5′ and 0° 10′, respectively. Approximately one third of the experimental points were observations made at negative angles. A sufficient number of counts were accumulated in both the monitor and elastic detectors to give approximately a 2% statistical error in the determination of yield.

[11] Model 8; Manufactured by Manostat Corporation, New York, New York.

After appropriate dead-time corrections were applied to the elastic and monitor detectors, the differential cross section was calculated from the yield by means of the geometrical factor of Critchfield and Dodder.[12] In using this expression account is taken of the finite divergence of the beam by assuming that the nickel window acts as a uniform isotropic source of particles. Should the target volume be a section of a cylinder rather than the frustrum of a cone, however, these data would be overcorrected, i.e., low, by approximately 3.5%. It is felt that the description chosen represents the actual conditions much more closely. The relative derivatives of the true cross section, σ'/σ and σ''/σ, used in the calculation of the G factor were approximated by the relative derivatives of the uncorrected cross section.

The energy of the beam at the detector was determined from a knowledge of the ratio of the pulse height of the elastic peak to the pulse height of the ThC′ alpha.[13] To obtain the energy at the target volume, the curves of Roll and Steigert[14] for the residual ranges vs energy of heavy ions in oxygen were differentiated to obtain the specific energy loss. The energy loss was then calculated from the relationship

$$\frac{d(E/A)}{\rho dx} \propto \frac{Z'}{A'} \ln\left(\frac{EK}{A\bar{I}}\right),$$

where ρ, A', Z' are the density, atomic number, and nuclear charge of the stopping material, respectively, and E/A is the energy per amu of the incident particle. The average ionization potential was taken to be 13 Z' ev.[15] Since the reference material is gaseous and the difference in Z' small, the specific energy losses calculated in this way are believed to be accurate to better than 2% for the region in which they are used here.

No corrections for either multiple or slit-edge scattering have been applied to these data. An estimate of the multiple scattering which results in a measured yield greater than the true yield was made, however. The increased yield is proportional (in first approximation) to the product of the relative second derivative of the cross section times the mean square deviation of the Gaussian portion of the scattering distribution.[16]

At laboratory angles of 3°, 6°, and 10° this amounts to approximately 3%, 0.7%, and 0.2%, respectively. An estimate of the slit-edge scattering is placed at 0.2%.

Table II is a summary of the estimated experimental errors. The combined effect of these uncertainties is to assign a relative error of ±4% to these data. The standard error in the absolute magnitude of the differential cross section is taken to be ±15%.

TABLE II. Estimated experimental errors.

Source	Angular region (lab) 2°–5°	5°–10°
Alignment[a]	2.5%	1.8%
G factor	0.5%	1.5%
Counting statistics	2.0%	2.0%
Counting loss	0.02%	0.02%
Target density	1.5%	1.5%
Angle	0.5′	0.5′
Energy	2.0%	2.0%
Beam current	15.0%	15.0%

[a] Includes uncertainties in the aperture and interaperture dimensions.

RESULTS AND DISCUSSION

The results of this experiment are presented graphically as the ratio of the observed differential cross section to Rutherford vs the center-of-mass angle. One may note that as η is increased from ~1 to ~4 the amplitude of the diffraction-like oscillations decrease markedly and the drop below Rutherford slowly becomes more pronounced.

Since all results show diffraction-like effects to some varying degree and the penetration depth for heavy ions in nuclear matter is expected to be very slight, the experimental results are compared with the predictions of a simple diffraction calculation. The diffraction pattern for an opaque sphere may be expressed in terms of the first-order cylindrical Bessel function. The argument is taken as $\beta=2kR\sin(\theta/2)$, where k is the center-of-mass wave number, R the interaction radius and θ the center-of-mass scattering angle. The differential cross section may be expressed as[8]

$$d\sigma/d\Omega = k^2R^4\cos^2(\theta/2)[J_1(\beta)/\beta]^2.$$

In general, although the locations of the maxima and minima are described, the predicted cross sections are too low for small angles and too great for larger angles.

The sharp-cutoff model is valid if η is much larger than unity. Also, it has been observed that in α-particle scattering[17] the model breaks down where $\sigma/\sigma_{\text{Coul}}<1/\eta$. In view of the fact that the majority of these data fail to satisfy one or both of the restrictions, it is not surprising that the over-all fit is rather poor.

The modified Blair model prediction for the differential scattering cross section relative to Coulomb without a nuclear phase shift term but including an amplitude factor for the lth partial wave may be written as

$$\frac{\sigma}{\sigma_c} = \left|\sin(\eta\ln B) + \frac{B}{\eta}\sum_{l=0}^{\infty}(2l+1)P_l(\cos\theta)(1-A_l)\cos 2\sigma_l + i\left[\cos(\eta\ln B) + \frac{B}{\eta}\sum_{l=0}^{\infty}(2l+1)P_l(\cos\theta)(1-A_l)\sin 2\sigma_l\right]\right|^2,$$

[12] C. L. Critchfield and D. C. Dodder, Phys. Rev. **75**, 419 (1949).
[13] E. Newman and F. E. Steigert, Phys. Rev. **118**, 1575 (1960).
[14] P. G. Roll and F. E. Steigert, Nuclear Phys. **16**, 534 (1960).
[15] R. M. Sternheimer, Phys. Rev. **115**, 137 (1959).
[16] B. Rossi and K. Greisen, Revs. Modern Phys. **13**, 267 (1941).
[17] H. E. Wegner, R. M. Eisberg, and G. Igo, Phys. Rev. **99**, 825 (1955).

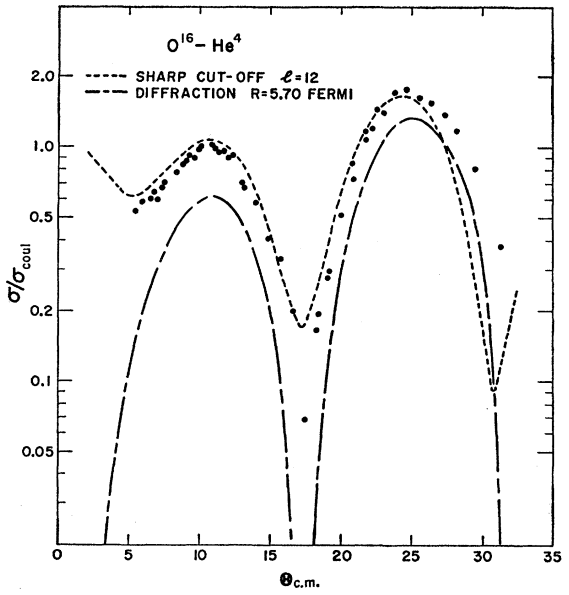

FIG. 3. Elastic scattering of O^{16} by He^4. The energy in the center-of-mass system at the target volume is 32.2 Mev. Results of a diffraction and sharp cutoff calculation are shown.

where

$$B=\sin^2(\theta/2),$$

$$\sigma_l=\sum_{l''=1}^{l}\tan^{-1}(\eta/l'').$$

The amplitude is taken to be

$$1-A_l=\frac{1}{1+\exp[(l-L)/\Delta l]}.$$

The result is a Saxon-shaped edge, where L (the sharp cutoff l resulting in the best fit to the locations of the maxima and minima) is the half-amplitude l value and Δl is the diffuseness parameter. The "thickness" ΔR of the nuclear edge may then be expressed as

$$\Delta R=R_{L+\Delta l}-R_{L-\Delta l}.$$

The modified-cutoff model used here is similar to that introduced by McIntyre *et al.*,[4] with the exception that the rounding of the nuclear phase shift has been omitted.

$O^{16}-He^4$

The observed differential cross section divided by the Coulomb cross section vs the center-of-mass angle θ for O^{16} on He^4 is shown in Fig. 3. The energy at the target in the c.m. system is 32.2 Mev. It may be noted that this reaction is inverted in the sense that usually oxygen is bombarded with alpha particles. There are no advantages to the order chosen other than the improved detector energy resolution. Compensating for this gain, however, is a loss of angular resolution in the center-of-mass system. This effect poses no serious problem here because of the width of the diffraction structure. By performing the experiments in this inverted order, the accuracy of the very small angle data (2° lab) could be checked against the published data of Yavin and Farwell.[18] Although the energy at the target is not stated, the center-of-mass energy should be only slightly different than that of the present experiment. The first minimum and succeeding maximum detected by these workers are exactly duplicated in angle by the dip at $\theta=17.5°$ and the peak at 24° found in this experiment. Their measurements were not carried to sufficiently small an angle to observe the peak at 11° now reported.

The ratio of the cross sections for the 24° peak is shown as approximately 1.0 in reference 18. The ratio in the present work is ~1.0 for the 11° peak and 1.75 for the succeeding maximum. This increase in the ratio of observed to Coulomb cross section for succeeding maxima has been observed previously in the elastic scattering of alpha particles from carbon.[19] The difference in the absolute cross section for the 24° peak is greater than the quoted limits of error for the two experiments. It should be pointed out, however, that Aguilar *et al.*[20] have also investigated this reaction at an energy of 30.4 Mev (c.m.) and find a value of 1.9 for this ratio.

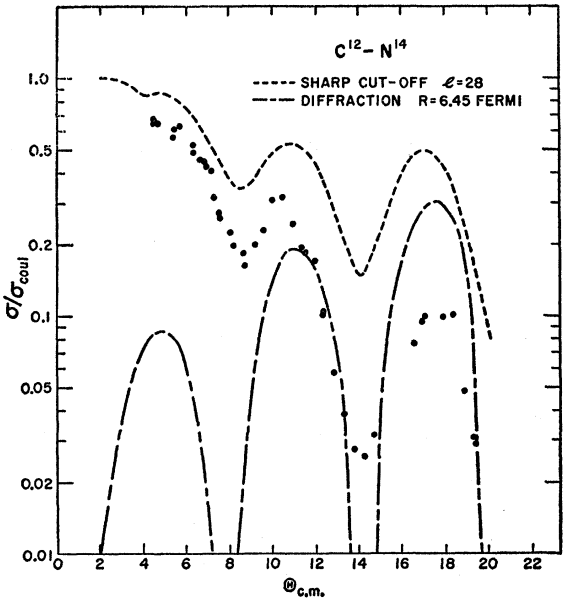

FIG. 4. Elastic scattering of C^{12} by N^{14}. The energy in the center-of-mass system is 62.5 Mev. Predictions of the simple diffraction model and the sharp-cutoff model are also shown.

[18] A. I. Yavin and G. W. Farwell, Nuclear Phys. **12**, 1 (1959).
[19] G. Igo, H. E. Wegner, and R. M. Eisberg, Phys. Rev. **101**, 1508 (1956).
[20] J. Aguilar, W. E. Burcham, J. Catala, J. B. A. England, J. S. C. McKee, and J. Rotblat, Proc. Roy. Soc. (London) **A254**, 395 (1960).

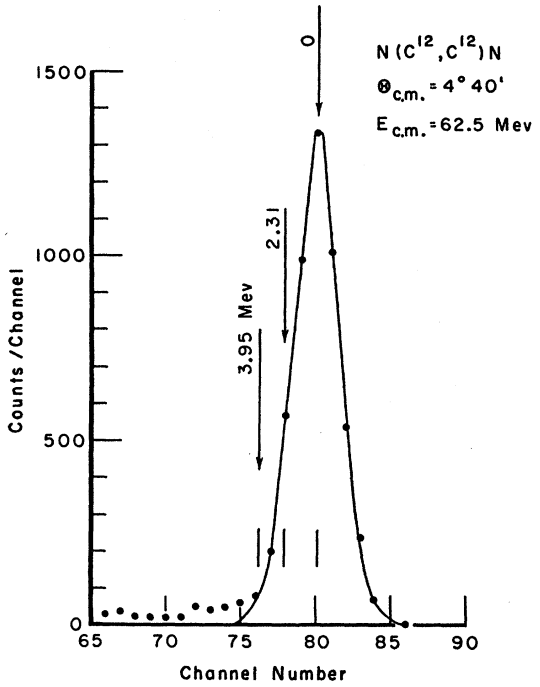

FIG. 5. Elastic detector spectrum for the scattering of C^{12} by N^{14}. The resolution is sufficient to eliminate all excited states with the exception of the first excited state of N^{14}.

No attempt was made to follow the angular distribution of the inelastic scattering from the first and second excited states of O^{16}. An estimate of the cross section at the 17.5° minimum was made; it is approximately 50% of the elastic scattering section at this angle, in agreement with the results of reference 18.

The results of a diffraction calculation and of a sharp-cutoff calculation are also shown in Fig. 3. The interaction radii obtained from these fits are 5.70 and 5.97 fermi, respectively. The results of a modified cutoff could not be applied to this case since the effect of the modification as used here is to decrease the peak-to-valley ratio and an increase is required.

$C^{12}-N^{14}$

The results of the scattering of C^{12} by nitrogen (99.6% N^{14}) are shown in Fig. 4. The values of η and the c.m. energy are 2.09 and 62.5 Mev, respectively. The results of a diffraction and sharp cutoff calculation with interaction radii of 6.45 and 6.99 f, respectively, are also shown. It is seen that, although one may obtain a fit to the location of the maxima, the predicted cross sections do not reproduce the experimental data very satisfactorily. The Blair model predicts cross sections consistently larger than those observed. In addition the peak-to-valley ratios are less than the measured ones, thus, as in the O-He case, ruling out the application of the modified model.

The elastic detector spectrum from the 400-channel analyzer is shown in Fig. 5. All excited states of C^{12} and all but the first excited state of N^{14} are clearly resolvable. One would expect no contribution from this state since scattering from this level requires violation of the conservation of isotopic spin. Within the statistical accuracy of the points in the elastic scattering spectra no asymmetry was noted in the elastic peak.

$O^{16}-N^{14}$

In Fig. 6 are presented the results of the elastic scattering of O^{16} by N^{14}. The diffraction structure for this reaction oscillates with considerably smaller amplitude than the previous cases. Maxima are seen to occur at 9° 30′, 14° 35′, and 19° 50′. The cross section rises to approximately 1.5 times the Coulomb value in the neighborhood of 5 deg. A rerun of the absolute calibration using a slightly different geometry duplicated the original measurement to better than 5%. Once again the predictions of the diffraction and sharp-cutoff models fail to correspond to the data in anything but phase. The interaction radii inferred are 6.80 and 7.21 f, respectively. The results of a modified calculation are applicable here since the observed peak-to-valley ratio is less than that expected from the sharp-cutoff model. The solid line in Fig. 6 shows this result for $l=33$ and $\Delta l=1.3$. The value of Δl shown was chosen as best representing the amplitude of the diffraction structure. It should be noted, however, that to fit the majority of the data it was required that the theoretical cross section be multiplied by a factor of 0.6. The ΔR obtained in this way is 0.51 f or 7.1% of the mean radius.

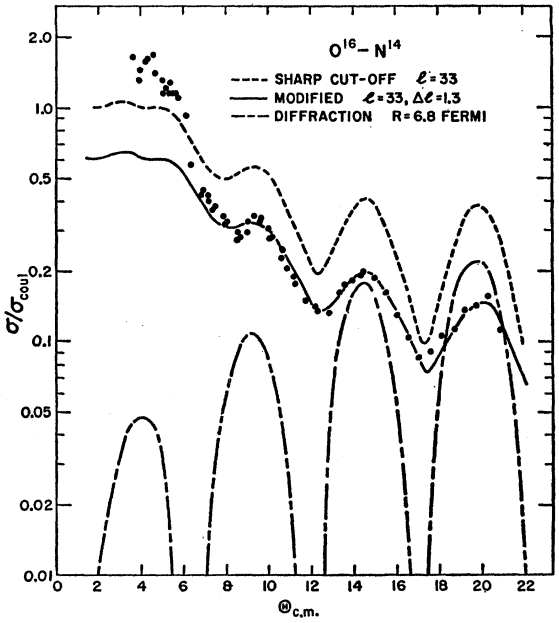

FIG. 6. Elastic scattering of O^{16} by N^{14}. The results of the diffraction and sharp-cutoff calculations are shown; the modified cutoff prediction has been normalized to reproduce the data beyond 6 deg.

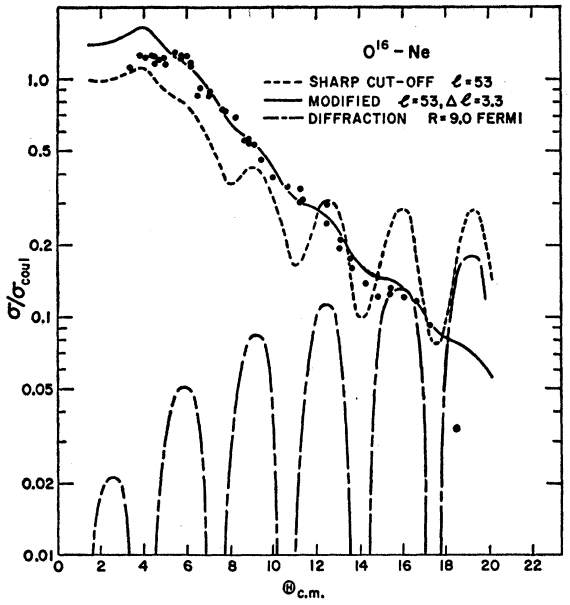

FIG. 7. Elastic scattering of O^{16} by Ne. The diffraction and sharp-cutoff predictions are shown. The results of a modified-cutoff calculation have been normalized to the observed data.

As in the $C^{12}-N^{14}$ case the only excited state that is not completely resolvable is the 2.31-Mev first excited state of N^{14}. As discussed in the previous section, it follows from the law of conservation of isotopic spin that this state would not be expected to contribute. Once again no asymmetry of the elastic peak was noted.

$O^{16}-Ne$

The ratio of the absolute differential cross section to the Coulomb cross section vs the center-of-mass angle for the elastic scattering of O^{16} from neon (90.9% Ne^{20}, 0.26% Ne^{21}, and 8.8% Ne^{22}) is shown in Fig. 7. The diffraction structure is almost completely washed out. The value of η is 3.9 and the energy in the center of mass is 87.0 Mev for Ne^{20}.

The radii inferred from the diffraction and Blair models are 9.0 and 9.48 f, respectively. The uncertainty in locating the peaks and valleys in the diffraction structure leads to an ambiguity of approximately 0.1 f. A modified calculation with $l=53$, $\Delta l=3.3$ is shown in Fig. 7, normalized so as to best reproduce the data.

TABLE III. Parameters and nuclear radii for the reactions studied.[a]

Reaction	η	$E_{c.m.}$ (Mev)	R_{diff}	$(r_0)_{diff}$	$R_{s.c.}$	$(r_0)_{s.c.}$	ΔR
$O^{16}-He^4$	0.80	32.2	5.70	1.39	5.97	1.45	···
$C^{12}-N^{14}$	2.09	62.5	6.45	1.37	6.99	1.49	···
$O^{16}-N^{14}$	2.70	71.7	6.80	1.38	7.21	1.46	0.51
$O^{16}-Ne^{20}$	3.90	87.0	9.00	1.72	9.48	1.81	1.08

[a] All radii are in fermi.

A ΔR of 1.08 f (11.4% of the mean radius) is found from the diffuseness parameter.

The resolution of the elastic detector (3.3 Mev full width at half-maximum) is sufficient to resolve all levels with the exception of the 1.63-Mev first excited state of Ne^{20}. Although no asymmetry of the elastic peak was observed, an upper limit of 10% is placed on the undetectable contribution of this state to the elastic scattering cross section.

CONCLUSIONS

Table III lists the values of the parameters and the nuclear radii obtained from this experiment. Included also are the values of r_0 determined from the diffraction and sharp-cutoff models, where

$$R=r_0(A_1^{\frac{1}{3}}+A_2^{\frac{1}{3}}).$$

It may be seen that the radii obtained by the sharp cutoff are larger in each case than those obtained from the diffraction model. One also notes that the r_0 value for the $O^{16}-Ne$ reaction is abnormally large, but the diffuseness of the nuclear edge is also correspondingly greater. Although obviously more information is needed it seems reasonable to conclude that the modified model, as used here, is not applicable to reactions when η is less than ~ 2.5.

ACKNOWLEDGMENTS

The authors wish to extend their thanks to J. G. Kelly for his assistance in collecting these data and to the staff and operators of the heavy-ion accelerator for their efforts. It is also a pleasure to thank the members of the Electronuclear Research Division at ORNL for their help and interest and for providing the IBM-704 computing time.